Adaptive fault accommodation of pitch actuator stuck type of fault in floating offshore wind turbines

A subspace predictive repetitive control approach

Liu, Yichao; Frederik, Joeri; Fontanella, Alessandro; Ferrari, Riccardo M.G.; Van Wingerden, Jan Willem

DOI
10.23919/ACC45564.2020.9147695

Publication date
2020

Document Version
Final published version

Published in
Proceedings of the American Control Conference, ACC 2020

Citation (APA)
Liu, Y., Frederik, J., Fontanella, A., Ferrari, R. M. G., & Van Wingerden, J. W. (2020). Adaptive fault accommodation of pitch actuator stuck type of fault in floating offshore wind turbines: A subspace predictive repetitive control approach. In *Proceedings of the American Control Conference, ACC 2020* (pp. 4077-4082). IEEE. https://doi.org/10.23919/ACC45564.2020.9147695

2020 American Control Conference
Denver, CO, USA, July 1-3, 2020

Adaptive fault accommodation of pitch actuator stuck type of fault in floating offshore wind turbines: a subspace predictive repetitive control approach*

Yichao Liu[1], Joeri Frederik[1], Alessandro Fontanella[2], Riccardo M.G. Ferrari[1] and Jan-Willem van Wingerden[1]

Abstract— **Individual Pitch Control (IPC) is a well-known and, in normal operating conditions, effective approach to alleviate blade loads in wind turbines. However, in the case of a Pitch Actuator Stuck (PAS) type of fault, conventional IPC is not beneficial since its action is disturbed by the failed pitch actuator. In this paper, a Subspace Predictive Repetitive Control (SPRC)-based IPC is proposed to implement a Fault Tolerant Control (FTC) strategy for Floating Offshore Wind Turbines (FOWTs) affected by PAS faults. In particular, an online subspace identification step is first carried out to obtain a linearized model of the FOWT system in faulty condition. The identified FOWT system is then used to develop a repetitive control law. Consequently, the adaptive repetitive control solution is implemented on the remaining healthy pitch actuators, in order to accommodate the PAS fault. Results show the developed SPRC approach allows to accommodate the PAS faults, achieving a considerable reduction of the blade loads in combination with lower pitch activities for the healthy actuators. This allows to continue power production and postpone maintenance operations, thus reducing the O&M costs.**

I. Introduction

Offshore wind has gained substantial attention over the past decade as one of the most promising renewable energy resources [1]. In the campaign of the offshore wind exploitation, the Floating Offshore Wind Turbine (FOWT) becomes the ideal alternative to bottom-fixed solutions for harvesting the deep-water wind resources [2].

However, FOWTs may experience unexpected mechanical and electric faults because of the harsh environmental conditions in which they have to operate and of the limited access possibility for maintenance [3]. In particular, the pitch and hydraulic systems, which play a critical role in optimizing the power generation, mitigating operational loads, stalling and aerodynamic braking, make up the biggest portion (around 13%) of the overall failure rate for offshore wind turbines [4]. Therefore, the reliability, safety and resilience of the pitch and hydraulic systems have received considerable attention in the study and development of FOWTs [5].

The pitch and hydraulic systems might experience *severe* faults, such as Pitch Actuator Stuck (PAS), which will lead to a complete loss of control authority, as well as *non-severe* ones, such as pitch actuator or sensor degradation [6]. Currently the preferred way for dealing with a PAS once it is successfully detected is via a safe and fast shutdown of the wind turbine. However, as PAS faults may occur frequently [7], such a policy is likely to lead to high Operation and Maintenance (O&M) costs due to lost power production and unplanned maintenance. These reasons make it urgent to develop a FTC approach that could: 1) accommodate the PAS, 2) prevent further deterioration of the faulty system and 3) make it possible to continue power production until the next planned maintenance.

The goal of this paper is to propose a novel adaptive FTC solution for FOWTs, that shall reduce blades loads in nominal healthy conditions and accommodate PAS faults. To pursue this goal, a so-called *Subspace Predictive Repetitive Control* (SPRC) strategy is introduced. It is based on the online solution, at every time step, of two problems. The first one consists in identifying a linear model of the FOWT dynamics at frequencies of interest, via online subspace identification. In particular, a contribution of the present paper is an extension that allows to identify the model even in faulty conditions. The second problem uses the online identification results for generating an individual pitch control (IPC) law, based on the Repetitive Control (RC) approach. The solution is such that the blade loads are minimized in both healthy and faulty conditions. The effectiveness of the proposed adaptive FTC with the SPRC-based IPC is illustrated via a numerical study involving a 10MW FOWT benchmark [8].

The remainder of the paper is organized as follows. Section II introduces the 10MW FOWT and the simulation environment. In section III, the SPRC approach of the IPC is detailed. Next, a numerical simulation using the Fatigue, Aerodynamics, Structures, and Turbulence (FAST) simulator is implemented in section IV. Section V presents concluding remarks.

II. Description of the 10MW FOWT and of the fault scenario

In this section, the FOWT model considered as reference in the present paper is described. It is based on the DTU 10MW three-bladed variable speed reference wind turbine and the Triple-Spar floating platform [8]. The block diagram for the 10MW FOWT simulation model is portrayed in Fig. 1. It comprises an aero-hydro-structural dynamic part simulated in the well known FAST numerical package [9]

*This research was supported by the European Union via a Marie Sklodowska-Curie Action (Project EDOWE, grant 835901). [1]Delft University of Technology, Delft Center for Systems and Control, Mekelweg 2, 2628 CD Delft, The Netherlands. {Y.Liu-17, J.A.Frederik., R.Ferrari, J.W.vanWingerden}@tudelft.nl. [2]Politecnico di Milano, Mechanical Engineering Department, Via La Masa 1, 20156, Milano, Italy. {alessandro.fontanella}@polimi.it.

978-1-5386-8266-1/$31.00 ©2020 AACC

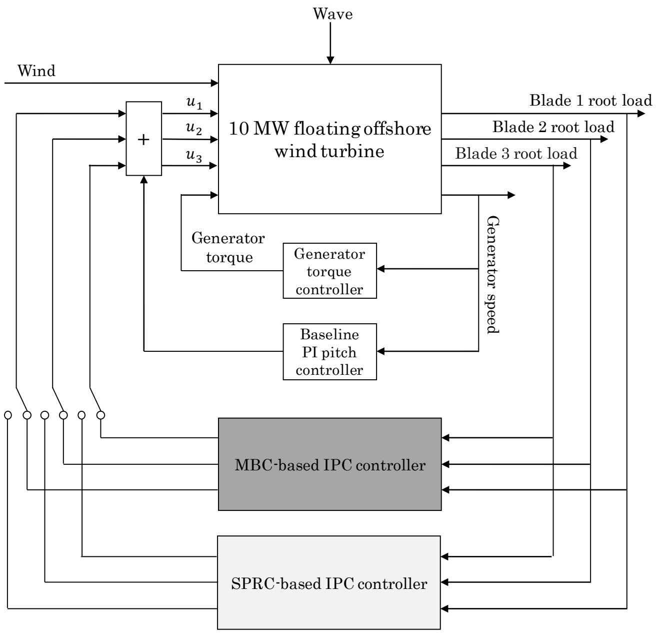

Fig. 1. Block scheme of the controller and loop of the 10MW FOWT.

and a wind turbine control part implemented in *MathWorks Simulink*. Specifically, the pitch control can be divided into 1) Baseline control utilizing the classical Collective Pitch Control (CPC) [8], which encompasses the white block, 2) Multi-Blade Coordinate (MBC)-based IPC [10], which is represented by the dark grey block, 3) SPRC-based IPC, which is characterized by a light grey block and would be introduced in section III.

As for the aero-hydro-structural dynamic part, the FOWT will be characterized by the following discrete-time system,

$$\begin{cases} x_{k+1} &= A^0 x_k + \rho(x_k, u_k) + \\ & \quad \beta_{k-k_0}\Phi_k^x(u_k, \vartheta^x) + \eta_k^x(x_k, u_k, k) \\ y_k &= C^0 x_k \end{cases}, \tag{1}$$

where $k = 0, 1, \ldots$ is the discrete time index and $x \in \mathbb{R}^n$, $u \in \mathbb{R}^r$, $y \in \mathbb{R}^l$ represent the state, the control input and the measurement output vectors, respectively. Vector u collects the three pitch commands, y the three blades Out-of-Plane (OoP) bending moment. The matrix $A^0 \in \mathbb{R}^{n\times n}$ and the vector field $\rho : \mathbb{R}^n \times \mathbb{R}^r \mapsto \mathbb{R}^n$ denote the linear and nonlinear parts of the FOWT nominal (i.e. relative to healthy conditions) dynamics while $C^0 \in \mathbb{R}^{l\times n}$ is the nominal output matrix. The unavoidable modelling uncertainties and periodic disturbances induced by wind loading are described by $\eta_k^x : \mathbb{R}^n \times \mathbb{R}^r \times \mathbb{R} \mapsto \mathbb{R}^n$.

β_{k-k_0} is the time profile of the fault, where k_0 is the faulty time index. The term $\beta_{k-k_0}\Phi_k^x(u_k, \vartheta^x)$ represents the changes of the dynamics of the state equation, due to the occurrence of the PAS type of faults. The PAS is modelled by the following equation,

$$\Phi_k^x = -u_k + \vartheta^x \varepsilon\,, \tag{2}$$

where ϑ^x denotes the value of pitch angle of the f^{th} blade induced by the actuator stuck while ε represents an all zeroes column vector of suitable size having a single 1 in its f^{th} position. In addition, it is assumed that only one blade is stuck in each case study.

III. Adaptive fault accommodation with SPRC

The FOWT system dynamics in equation (1), can be approximated by an LTI system affected by unknown periodic disturbances [11] in prediction form as,

$$\begin{cases} x_{k+1} &= \tilde{A}x_k + B(u_k + \Phi_k^x) + \tilde{E}d_k + Ly_k \\ y_k &= Cx_k + Fd_k + e_k \end{cases}, \tag{3}$$

where d_k denotes the periodic component of disturbances on the blades, $e_k \in \mathbb{R}^l$ is the aperiodic component of the blade loading.

Furthermore, $\tilde{A} \triangleq A - LC$ and $\tilde{E} \triangleq E - LF$, where matrices $A \in \mathbb{R}^{n\times n}$, $B \in \mathbb{R}^{n\times r}$, $C \in \mathbb{R}^{l\times n}$, $L \in \mathbb{R}^{n\times l}$, $E \in \mathbb{R}^{n\times m}$ and $F \in \mathbb{R}^{l\times m}$ are the state transition, input, output, observer, periodic noise input and periodic noise direct feed-through matrices, respectively. During healthy conditions ($0 \le k < k_0$), it holds $\Phi_k^x = 0$.

By defining a periodic difference operator δ, the effect of the periodic disturbance on the input-output system could be eliminated:

$$\begin{aligned} \delta d_k &= d_k - d_{k-P} = 0, \\ \delta u_k &= (u_k + \Phi_k^x) - (u_{k-P} + \Phi_{k-P}^x), \\ \delta y_k &= y_k - y_{k-P}, \end{aligned}$$

with P being the disturbance period. During the occurrence of a PAS type of fault, δu for the f^{th} blade is 0, since $\Phi_k^x = \Phi_{k-P}^x$ accordingly.

Based on the definition of δ, equation (3) is formulated as

$$\begin{cases} \delta x_{k+1} &= \tilde{A}\delta x_k + B\delta u_k + L\delta y_k \\ \delta y_k &= C\delta x_k + \delta e_k \end{cases} \tag{4}$$

If we consider a given time window of length p in the past, we can define the following stacked vector

$$\delta U_k^{(p)} = \begin{bmatrix} u_k - u_{k-P} \\ u_{k+1} - u_{k-P+1} \\ \vdots \\ u_{k+p-1} - u_{k+p-P-1} \end{bmatrix}, \tag{5}$$

and, similarly, the vector $\delta Y_k^{(p)}$. Then, the future state vector $\delta x_{(k+p)}$ can be introduced based on $\delta U_k^{(p)}$ and $\delta Y_k^{(p)}$ as

$$\delta x_{k+p} = \tilde{A}^p \delta x(k) + \begin{bmatrix} K_u^{(p)} & K_y^{(p)} \end{bmatrix} \begin{bmatrix} \delta U_k^{(p)} \\ \delta Y_k^{(p)} \end{bmatrix}, \tag{6}$$

where $K_u^{(p)}$ and $K_y^{(p)}$ are defined as,

$$\begin{aligned} K_u^{(p)} &= \begin{bmatrix} \tilde{A}^{p-1}B & \tilde{A}^{p-2}B & \cdots & B \end{bmatrix}, \\ K_y^{(p)} &= \begin{bmatrix} \tilde{A}^{p-1}L & \tilde{A}^{p-2}L & \cdots & L \end{bmatrix}. \end{aligned}$$

It is assumed that p is large enough such that $\tilde{A}^j \approx 0$ if $\forall j \ge p$ [12]. In such a case, δx_{k+p} is approximated by

$$\delta x_{k+p} = \begin{bmatrix} K_u^{(p)} & K_y^{(p)} \end{bmatrix} \begin{bmatrix} \delta U_k^{(p)} \\ \delta Y_k^{(p)} \end{bmatrix} \tag{7}$$

Combining equation (7) with (4), the approximation of $\delta\hat{y}_{k+p}$ is obtained as,

$$\delta y_{k+p} = \begin{bmatrix} CK_u^{(p)} & CK_y^{(p)} \end{bmatrix} \begin{bmatrix} \delta U_k^{(p)} \\ \delta Y_k^{(p)} \end{bmatrix} + \delta e_{k+p} \quad (8)$$

It is clear from equation (8) that the matrix of coefficients $\begin{bmatrix} CK_u^{(p)} & CK_y^{(p)} \end{bmatrix}$ contains all the necessary information on the behaviour of the FOWT system and can be estimated based on the input u and output y. We can now introduce the matrix $\Xi \in \mathbb{R}^{l\times((r+l)\cdot p)}$ containing the FOWT Markov parameters as,

$$\Xi = \begin{bmatrix} CK_u^{(p)} & CK_y^{(p)} \end{bmatrix} \quad (9)$$

Therefore, the aim of the identification is to find an online solution of the Recursive Least-Squares (RLS) optimization. In order to realize the adaptive control for the PAS type of fault, we will assume that the blade n load is independent of blade m, where $n \neq m$. Therefore, the subspace identification step for both healthy and faulty conditions is carried out by the following RLS optimization as,

$$\hat{\Xi}_{k,(i)} = \arg\min_{\hat{\Xi}_k} \sum_{k=0}^{\infty} \left\| \delta y_{k,(i)} - \lambda \hat{\Xi}_{k,(i)} \begin{bmatrix} \delta U_{k,(i)}^{(p)} \\ \delta Y_{k,(i)}^{(p)} \end{bmatrix} \right\|_2^2 , \quad (10)$$

where λ is a forgetting factor ($0 \ll \lambda \leq 1$) to attenuate the effect of past data, and adapt to the updated system dynamics online. In this paper, a large value, i.e. $\lambda = 0.99999$, was selected to guarantee the robustness of the optimization process (such value for λ corresponds to a window length of 10^6 samples [13]). In addition, $i = 1, 2, 3$ is the blade number, while $\hat{\Xi}_{k,(i)}$ denotes the estimate of independent Markov parameter for each blade. Consequently, the optimization process in equation (10) is conducted three times at each time instant k. Next, $\hat{\Xi}_k$ is synthesized as,

$$\hat{\Xi}_k = \begin{bmatrix} \hat{\Xi}_{k,(1)} \\ \hat{\Xi}_{k,(2)} \\ \hat{\Xi}_{k,(3)} \end{bmatrix} . \quad (11)$$

Based on the value $\hat{\Xi}_k$, the FOWT system dynamics are identified, taking into account the faulty conditions determined by the PAS occurrence. It is worth noticing that the FOWT system should be persistently excited in order to obtain a unique solution of the RLS optimization ([14]). Based on the identified $\hat{\Xi}_k$, the state feedback controller can be formulated by the following state-space representation, according to [15],

$$\underbrace{\begin{bmatrix} \bar{Y}_{j+1} \\ \delta\theta_{j+1} \\ \delta\bar{Y}_{j+1} \end{bmatrix}}_{\bar{K}_{j+1}} = \underbrace{\begin{bmatrix} I_{l\cdot P} & \phi^{+}\widehat{\Gamma^{(P)}K_u^{(P)}}\phi & \phi^{+}\widehat{\Gamma^{(P)}K_y^{(P)}}\phi \\ 0_{l\cdot P} & 0_{r\cdot P} & 0_{l\cdot P} \\ 0_{l\cdot P} & \phi^{+}\widehat{\Gamma^{(P)}K_u^{(P)}}\phi & \phi^{+}\widehat{\Gamma^{(P)}K_y^{(P)}}\phi \end{bmatrix}}_{\bar{A}_j} \underbrace{\begin{bmatrix} \bar{Y}_j \\ \delta\theta_j \\ \delta\bar{Y}_j \end{bmatrix}}_{\bar{K}_j} + \underbrace{\begin{bmatrix} \phi^{+}\hat{H}^{(P)}\phi \\ I_{r\cdot P} \\ \phi^{+}\hat{H}^{(P)}\phi \end{bmatrix}}_{\hat{B}_j} \delta\theta_{j+1} , \quad (12)$$

where $j = 0, 1, 2, \cdots$ is the rotation count. $\hat{H}^{(P)}$ and $\Gamma^{(P)}$ are the same matrices defined in [16]. $\theta \in \mathbb{R}^{2r}$ is the control inputs projected on the basis function Ψ which is defined in [17],

$$U_k^{(P)} = \Psi\theta_j , \quad (13)$$

where θ is updated at each P. The state transition and input matrices are updated at each discrete time instance k. Based on this, the classical optimal state feedback matrix $K_{f,j}$ can be synthesised in a Linear Quadratic Regulator (LQR) sense [18]. The control input vector $\delta\theta_j$ is then formulated according to the state feedback law,

$$\delta\theta_{j+1} = -K_{f,j}\bar{K}_j , \quad (14)$$

Considering that $\delta\theta_{j+1} = \theta_{j+1} - \theta_j$, the projected output update law θ_{j+1} can be calculated as,

$$\theta_{j+1} = \alpha\theta_j - \beta K_{f,j} \begin{bmatrix} \bar{Y}_j \\ \delta\theta_j \\ \delta\bar{Y}_j \end{bmatrix} , \quad (15)$$

where $\alpha \in [0, 1]$ and $\beta \in [0, 1]$ are the tuning parameters to increase the convergence rate of the algorithm. Finally, the input signals U_k can be computed by equation (13).

IV. Case Study

Now, the effectiveness of the proposed adaptive fault accommodation scheme is verified via a numerical study based on the 10MW FOWT model presented in section II.

A. Model configuration

As shown in Fig. 1, a 10MW FOWT model with twelve Degrees of Freedom (DOFs) was dynamically simulated in *FAST v8.16* [9] and coupled to *MathWorks Simulink*, where the wind turbine controllers were implemented. More specifically, we enabled in this simulation the DOFs of the generator, the 1st and 2nd flapwise blade modes, the 1st edgewise blade mode, the fore-aft and side-to-side tower bending modes as well as the six platform motions. The FOWT dynamics were studied under three different Load Cases (LCs). For the sake of verifying the control strategy, all of them were characterized by a constant and uniform wind field, analogously to [8]. The mean hub-height wind speed U_{hub} was set to 12, 16 and 20 m/s respectively. Furthermore, a specific PAS type of fault was chosen for the three LCs, considering a different pitch angle setting ϑ^x for the stuck blade, which in all cases was the third one (i.e. $f^{\text{th}} = 3$). The magnitude of ϑ^x was set to 20°, 0° and 10°, respectively. For each LC, 2000s were simulated with a fixed discrete time step of $T_s = 0.01$s, with the PAS fault always occurring at $t = $1000s.

Each LC was simulated alternatively implementing the proposed SPRC-based IPC and a MBC-based IPC. The performances of each control strategy in healthy and faulty conditions were evaluated according to their capacity to reduce the blade loads with respect to a baseline control implementing CPC.

In order to implement the online subspace identification part of the proposed SPRC-based IPC, a filtered pseudo-random binary signal with a maximum value of 3° is superimposed on top of the collective pitch demand of blades. This signal ensures persistence of excitation in the nominal healthy and faulty conditions and does not significantly affect the FOWT performances. Moreover, the value of past window p was selected as 21, in order to increase the convergence rate of the subspace identification.

B. Adaptive FTC with SPRC-based IPC

First of all, some time-domain plots are presented to illustrate the performance of the different controllers. Fig. 2 shows the comparisons of blade root Out-of-Plane (OoP) bending moments in LC2 for the two IPC control strategies, and for the CPC baseline. In the healthy condition before 1000s, both the MBC-based IPC and our SPRC-based IPC are able to effectively reduce the periodic blade loads. When a PAS fault occurs, the SPRC-based IPC does automatically start to learn the changed FOWT dynamics and adapt its control law, as explained in Section III. It is interesting to note that when the MBC-based IPC is implemented, the bending moments increase on the blade #1 and decrease on the blade #2 during the faulty condition. This makes the aerodynamics on the rotor more unbalanced: in particular, the bending moments on blade #2 drop into a negative value (around -1.5×10^4) due to the increased pitch angle from MBC-based IPC, as shown in Fig. 3. One plausible explanation is that the signals from the Coleman transformation utilized in the MBC-based IPC are contaminated by the failed pitch actuator and hence, the classical MBC-based IPC is not capable of reducing the loads, thus worsening the faulty condition.

Furthermore, the Power Spectral Densities (PSDs) of aforementioned OoP bending moments collected in the healthy condition (900s to 1000s) and the faulty condition (2900s to 3000s) are presented in Fig. 4. Both MBC-based IPC and SPRC-based FTC are able to effectively reduce the blade loads at 1P frequency in the healthy condition. However, the MBC-based IPC is unable to realize the load reduction in the faulty condition. Comparing to the MBC-based IPC approach, significant reductions of the OoP bending moments on the two healthy blades are achieved by the SPRC-based IPC when the third blade undergoes a PAS fault. More specifically, the dominant peak at 1P frequency (around 0.16Hz), caused by rotor imbalance, is reduced more effectively.

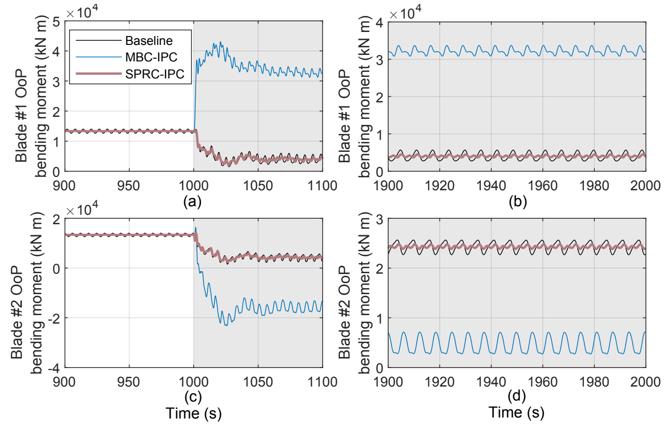

Fig. 2. Blade root OoP bending moments. (a)-(c) Simulation time from 900s to 1100s, (b)-(d) Simulation time from 1900s to 2000s. The faulty periods are indicated by a grey background. Blade #3 is not shown since it is the faulty blade.

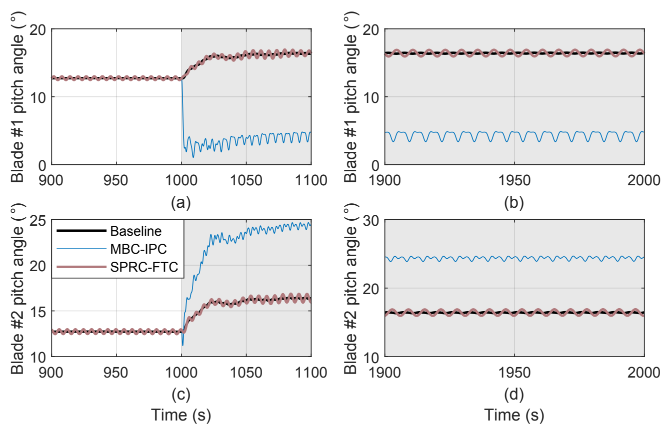

Fig. 3. Pitch angle of the blades. (a)-(c) Simulation time from 900s to 1100s, (b)-(d) Simulation time from 1900s to 2000. Time periods of faulty condition are indicated by a grey background. Blade #3 is not shown since it is the faulty blade.

In order to quantify the performance of the analyzed control strategies, Tab. I shows the load reduction with respect to baseline control in terms of standard deviation of the OoP bending moment for the considered three LCs. The standard deviation of the OoP bending moment for each blade was calculated considering only the part of the simulation from 900s to 1100s and from 1900s to 2000s. As anticipated, the proposed SPRC-based approach allows to reduce the loads induced by the unbalanced aerodynamics by more than 63% for the healthy blades thanks to its adaptive fault accommodation ability. The most significant load reduction (more than 83%) occurs in LC3, with highest wind and wave loads. This is an indication of the proposed approach capabilties to handle harsh wind and wave conditions even during a fault. In total, the aerodynamic loads on the rotor are reduced by more than 98% in all three LCs. Since the aerodynamic unbalance of the rotor is alleviated, the OoP bending moments on the faulty blade slightly decrease as

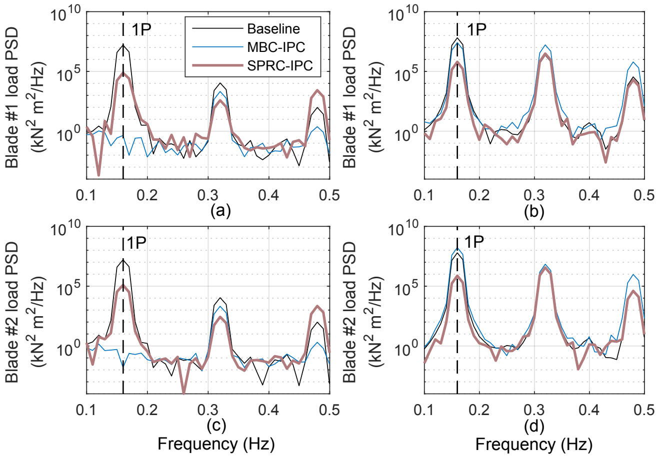

Fig. 4. Power spectrum density of the blade root OoP bending moments (a)-(c) Healthy condition from 900s to 1000s, (b)-(d) Faulty condition from 1900s to 2000. Blade #3 is not shown since it is the faulty blade.

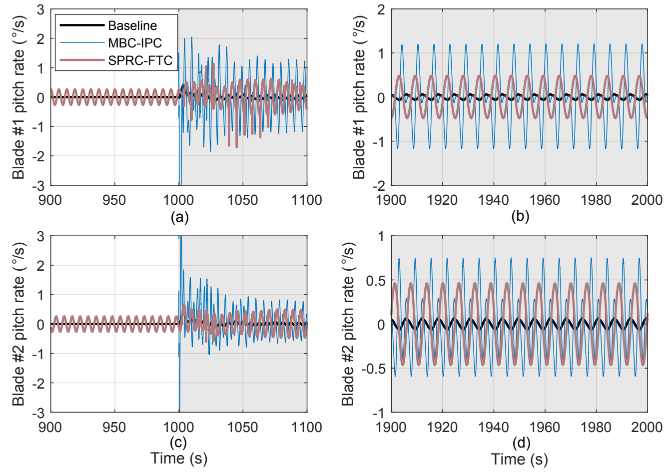

Fig. 5. Pitch rate of the blades. (a)-(c) Simulation time from 900s to 1100s, (b)-(d) Simulation time from 1900s to 2000. Time periods of faulty condition are indicated by a grey background. Blade #3 is not shown since it is the faulty blade.

TABLE I

COMPARISONS OF THE BLADE LOADS WITH DIFFERENT CONTROL STRATEGIES*.

Control strategies	Load case 1	Load case 2	Load case 3
Blade 1			
MBC-IPC (%)	55.90	20.00	10.48
SPRC-FTC (%)	63.74	76.29	83.04
Blade 2			
MBC-IPC (%)	*-36.80*	*-64.22*	20.72
SPRC-FTC (%)	64.02	74.01	88.36
Blade 3			
MBC-IPC (%)	30.94	*-7.48*	5.95
SPRC-FTC (%)	0.19	4.48	1.97
Cumulative loads			
MBC-IPC (%)	20.98	*-44.51*	*-54.81*
SPRC-FTC (%)	98.65	98.60	98.25

*The positive values indicate the percentage of the load reduction compared to the baseline control strategy.

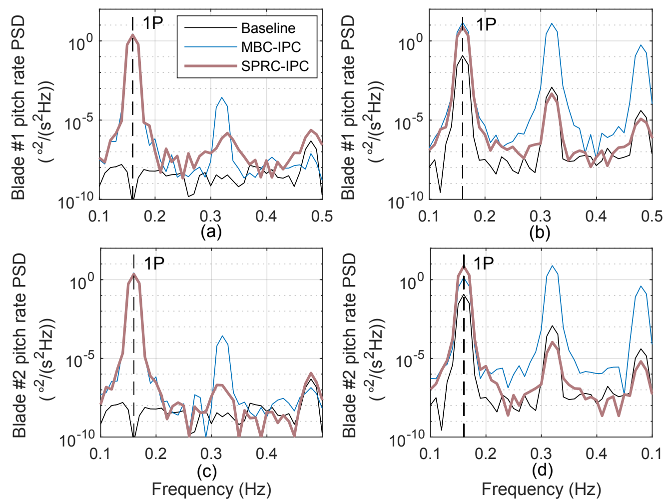

Fig. 6. Power spectrum density of the pitch rate. (a)-(c) Healthy condition from 900s to 1000s, (b)-(d) Faulty condition from 1900s to 2000. Blade #3 is not shown since it is the faulty blade.

well by around 0 to 4.5%. From the data in Tab. I it is also possible to notice that the standard deviation of the OoP moments is much higher when the MBC-based IPC is implemented. Especially, the italics implies the loads are increased by the MBC-based IPC and higher than baseline control. This implies that the classical IPC approach is not an effective way to deal with the PAS type of faults.

Moreover, it is found from Fig. 3 that the pitch angle commands set by the CPC vary much slower than with the IPC-based approaches. The effect of the SPRC-based IPC is to superimpose a periodic variation on top of the CPC pitch request, in order to reduce the loads induced by the PAS. It is also interesting to note that the control action of the MBC-based IPC is influenced by the PAS, resulting in a pitch angle request with a mean value different from the one of the CPC and SPRC-based IPC, which further deteriorates the faulty condition. The advantage of the SPRC-based IPC can be seen from the pitch rate presented in Figs. 5 and 6. The pitch rate demand is much lower than in the conventional IPC approach and it is strictly limited within the concerned 1P frequency. Actually, the effects of pitch rate are typically quantified by the Actuator Duty Cycle (ADC) indicator [19] which is an effective criterion to approximate the lifespan of pitch actuators. Smaller ADC values imply the reduced cyclic fatigue loads on the actuators and lower pitch activities. Fig. 7 presents the ADC for both nominal healthy conditions (i.e., 900s to 1000s) and faulty conditions (i.e. 1900s to 2000s) for the three LCs. As visible, the ADC of most blade pitches is, in general, reduced by the proposed SPRC-based approach by around 10% in healthy conditions and 19% in faulty conditions compared to the MBC-based IPC. Considering Fig. 5, it can be concluded that a significant amount of load mitigation during faulty conditions, which indeed is a form of fault tolerance, is achieved by the SPRC-based IPC without the need to increase pitching activities.

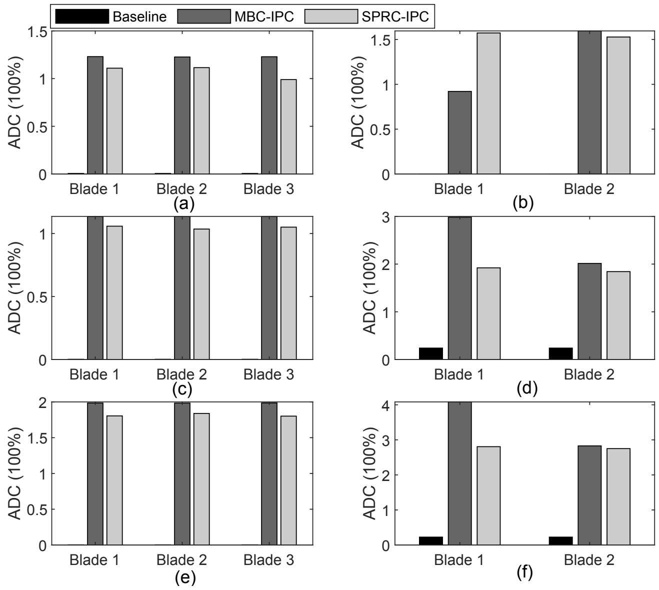

Fig. 7. ADC of the blade pitch actuator for the FOWT in healthy conditions (a)-(c)-(e) (simulation time from 900s to 1000s) in LCs 1, 2, 3 respectively and in faulty conditions, (b)-(d)-(f) (simulation time from 1900s to 2000s) in LCs 1, 2, 3 respectively.

V. Conclusions

Accommodating PAS type of faults in wind turbines poses huge challenges to control engineers on account of the reliability, safety and resilience of FOWTs. In the paper, we devise a novel adaptive FTC with SPRC, essentially an IPC combining online subspace identification with basis function learning control, to realize load reduction in the healthy conditions and automatically accommodate PAS faults in an adaptive way in the faulty conditions. Such an adaptive approach allows to realize significant load mitigation without priori knowledge from the turbine system and fault diagnosis architecture.

The effectiveness of the developed FTC with SPRC-based IPC is demonstrated through numerical simulations of a 10MW FOWT under different load cases. Results have shown that effective load alleviation is achieved in both nominal healthy and faulty conditions in an adaptive way with low pitch activities. More importantly, such a SPRC-based approach makes it possible to continue power production in faulty conditions, before maintenance can be performed.

References

[1] K. Ohlenforst, S. Sawyer, A. Dutton, B. Backwell, R. Fiestas, L. Joyce, L. Qiao, F. Zhao, and N. Balachandran, "Global wind statistics 2018," Global wind energy council, Report, 2019.
[2] M. Karimirad, *Offshore Energy Structures*. Springer International Publishing, 2014.
[3] J. Kang, L. Sun, and C. G. Soares, "Fault tree analysis of floating offshore wind turbines," *Renewable Energy*, vol. 133, pp. 1455 – 1467, 2019.
[4] J. Carroll, A. McDonald, and D. McMillan, "Failure rate, repair time and unscheduled o&m cost analysis of offshore wind turbines," *Wind Energy*, vol. 19, no. 6, pp. 1107–1119, 2016.
[5] Z. Jiang, M. Karimirad, and T. Moan, "Dynamic response analysis of wind turbines under blade pitch system fault, grid loss, and shutdown events," *Wind Energy*, vol. 17, no. 9, pp. 1385–1409, 2014.
[6] D. Li, P. Li, W. Cai, Y. Song, and H. Chen, "Adaptive fault-tolerant control of wind turbines with guaranteed transient performance considering active power control of wind farms," *IEEE Transactions on Industrial Electronics*, vol. 65, no. 4, pp. 3275–3285, 2018.
[7] J. Ribrant, "Reliability performance and maintenance—a survey of failure in wind power systems," Thesis, KTH School of Electrical Engineering, 2006.
[8] A. Fontanella, I. Bayati, and M. Belloli, "Linear coupled model for floating wind turbine control," *Wind Engineering*, vol. 42, no. 2, pp. 115–127, 2018.
[9] J. M. Jonkman and M. L. Buhl, "Fast user's guide," *SciTech Connect: FAST User's Guide*, 2005.
[10] S. P. Mulders, A. K. Pamososuryo, G. E. Disario, and J. W. van Wingerden, "Analysis and optimal individual pitch control decoupling by inclusion of an azimuth offset in the multiblade coordinate transformation," *Wind Energy*, vol. 22, no. 3, pp. 341–359, 2019.
[11] I. Houtzager, J. W. van Wingerden, and M. Verhaegen, "Wind turbine load reduction by rejecting the periodic load disturbances," *Wind Energy*, vol. 16, no. 2, pp. 235–256, 2013.
[12] A. Chiuso, "The role of vector autoregressive modeling in predictor-based subspace identification," *Automatica*, vol. 43, no. 6, pp. 1034 – 1048, 2007.
[13] F. Gustafsson, *Adaptive filtering and change detection*. Wiley, 2000.
[14] M. Verhaegen and V. Verdult, *Filtering and system identification: a least squares approach*. Cambridge university press, 2007.
[15] S. Navalkar, J. W. van Wingerden, E. van Solingen, T. Oomen, E. Pasterkamp, and G. van Kuik, "Subspace predictive repetitive control to mitigate periodic loads on large scale wind turbines," *Mechatronics*, vol. 24, no. 8, pp. 916 – 925, 2014.
[16] J. Frederik, L. Kröger, G. Gülker, and J. W. van Wingerden, "Data-driven repetitive control: Wind tunnel experiments under turbulent conditions," *Control Engineering Practice*, vol. 80, pp. 105–115, 2018.
[17] J. van de Wijdeven and O. Bosgra, "Using basis functions in iterative learning control: analysis and design theory," *International Journal of Control*, vol. 83, no. 4, pp. 661–675, 2010.
[18] R. Hallouzi, M. Verhaegen, R. Babuška, and S. Kanev, "Model weight and state estimation for multiple model systems applied to fault detection and identification," *IFAC Proceedings Volumes*, vol. 39, no. 1, pp. 648 – 653, 2006, 14th IFAC Symposium on Identification and System Parameter Estimation.
[19] C. Bottasso, F. Campagnolo, A. Croce, and C. Tibaldi, "Optimization-based study of bend–twist coupled rotor blades for passive and integrated passive/active load alleviation," *Wind Energy*, vol. 16, no. 8, pp. 1149–1166, 2013.